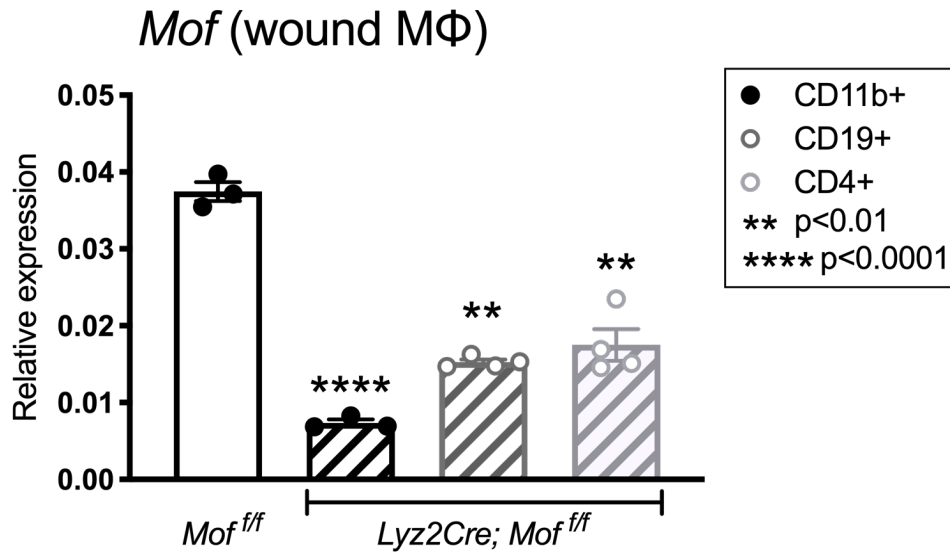
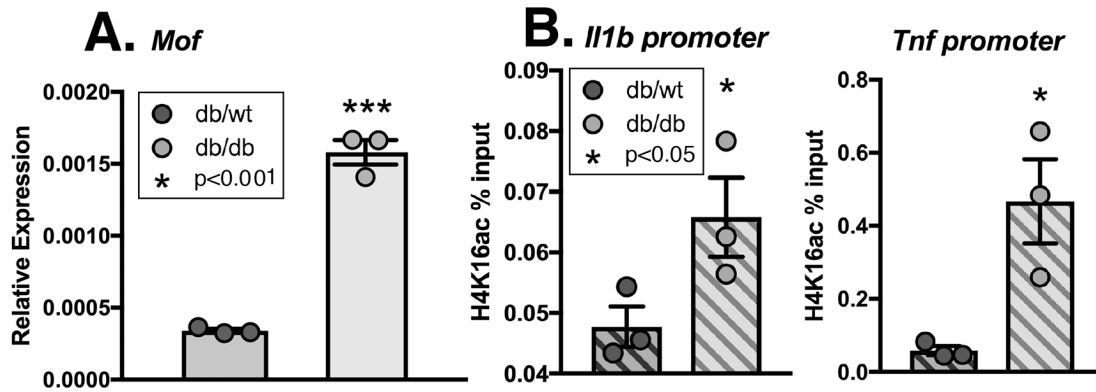


Supplemental Figures

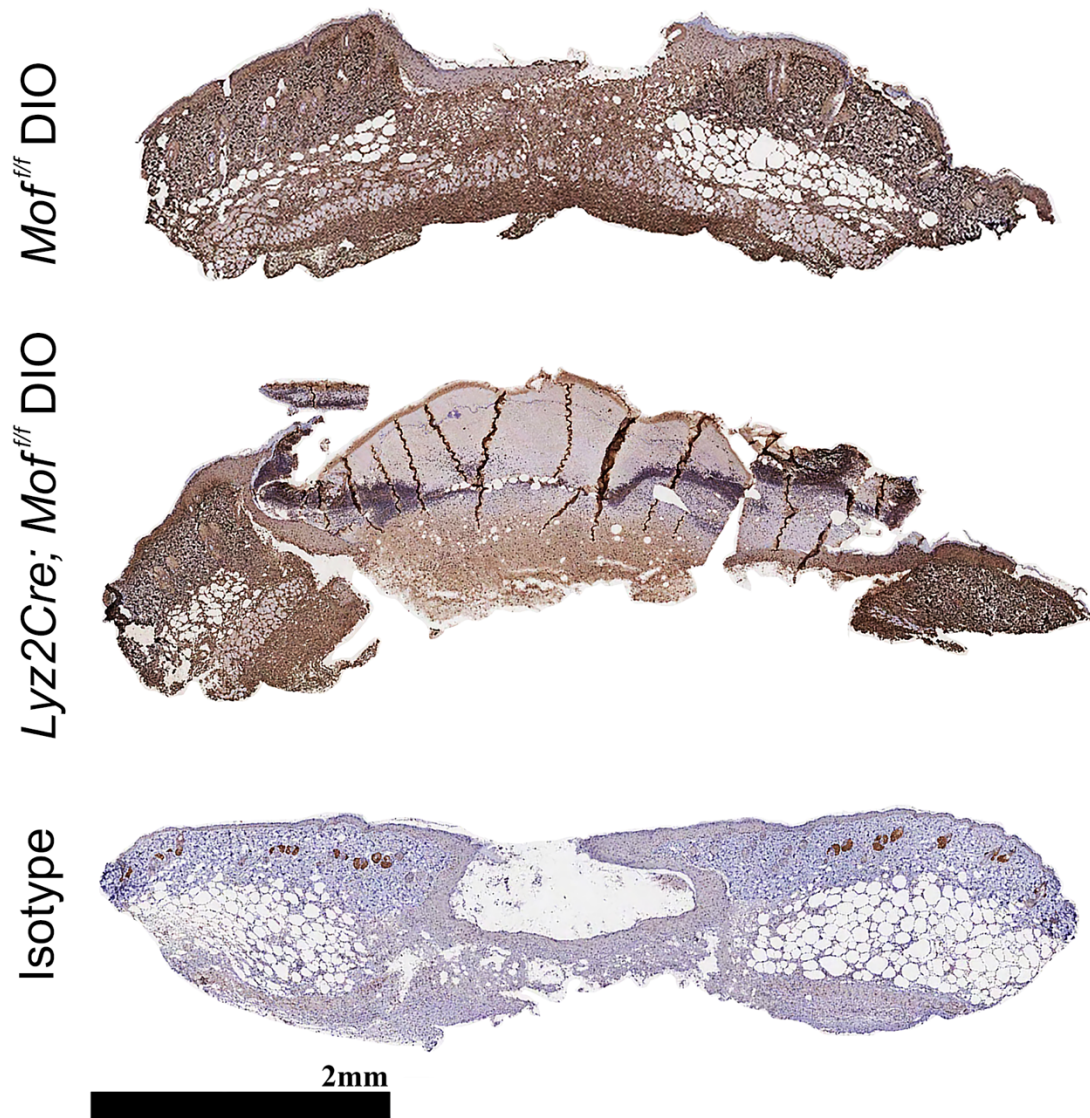


Supplemental Figure 1. *Mof* is specifically deleted in myeloid populations in

***Lyz2Cre;Mof*^{fl/fl} wounds.** Representative figure showing myeloid-specific deletion of *Mof* in *Lyz2Cre;Mof*^{fl/fl} wounds. Macrophages (CD11b⁺, n=3), B cells (CD19⁺, n=4), and T cells (CD4⁺, n=4) were FACS sorted from *Lyz2Cre; Mof*^{fl/fl} wounds harvested at day 5 post-wounding. *Mof* gene expression was measured by qPCR (n=3 mice pooled/replicate, repeated 2x). Data were analyzed using a 1-way ANOVA followed by Sidak's multiple comparison's test comparing each mean to *Mof*^{fl/fl} control CD11b⁺.



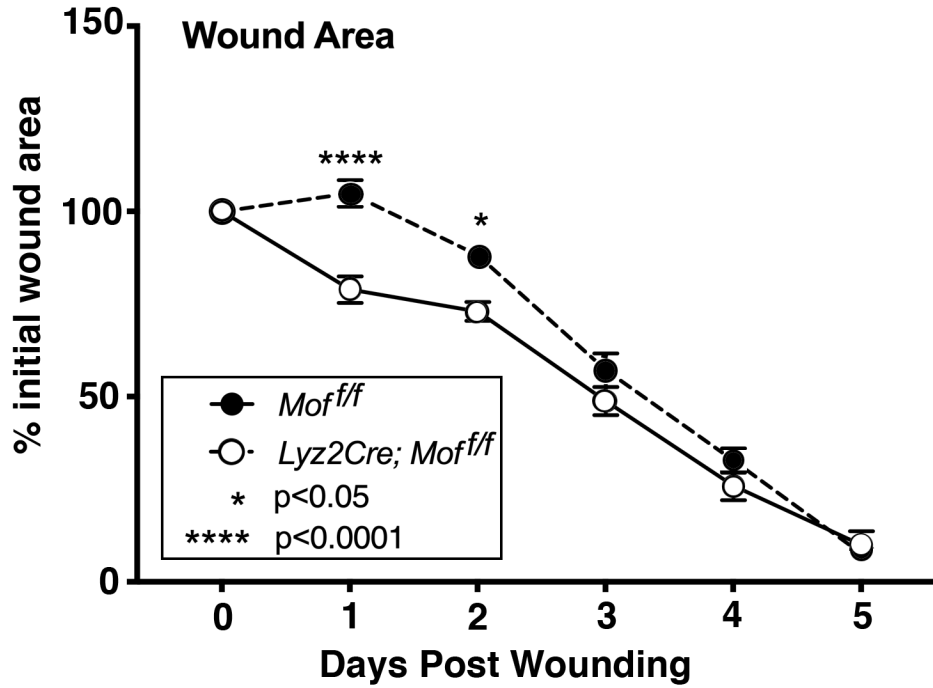
Supplemental Figure 2. MOF is elevated and H4K16ac is enriched on NFκB genes in db/db wound macrophages. A. Representative figure of *Mof* expression in db/db wound macrophages. Three wounds were created using a 6 mm punch on the backs of db/db or db/+ mice and wound macrophages (CD11b⁺CD3⁻ CD19⁻Ly6G⁻) were isolated on day 5 post-injury. *Mof* expression was measured by qPCR (n=3 x 3 mice pooled/replicate; repeated 2x). B. Representative figure showing increased H4K16ac deposition on inflammatory cytokine promoters. ChIP analysis was performed for H4K16ac at NFκB binding sites on the *Il1b* and *Tnf* promoters (n=3 x 4 mice pooled/replicate, repeated 2x). Data was analyzed using a 2-tailed Student's *t*-test.



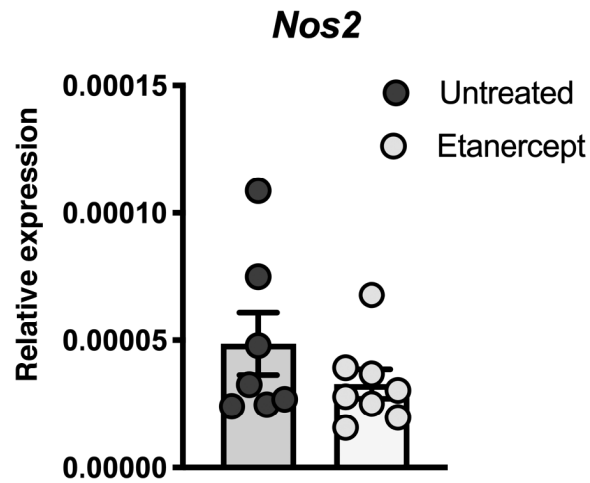
Supplemental Figure 3. Collagen deposition is increased in *Mof* deleted wounds.

Representative figures showing collagen deposition in day 5 *Lyz2Cre;Mof^{fl/fl}* DIO wounds.

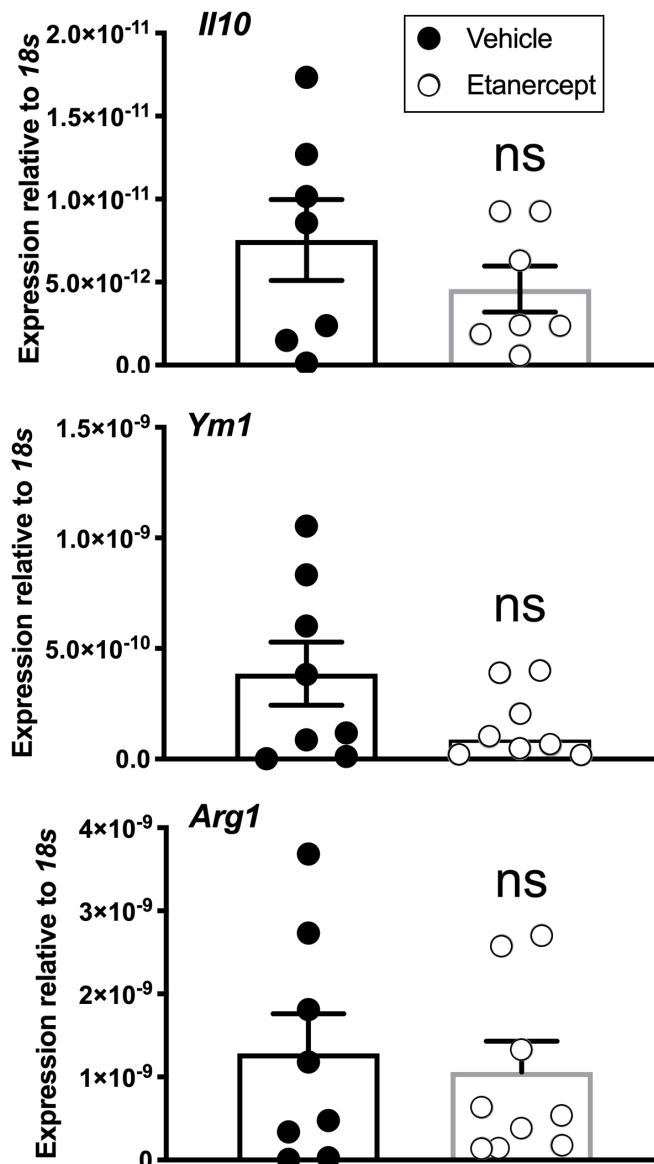
Wounds from DIO *Lyz2Cre; Mof^{fl/fl}* or DIO *Mof^{fl/fl}* mice were harvested on day 5 post-injury and processed for histology and stained using an antibody for collagen 1 (Rockland, 600-406-103) (n=6 mice/group). An isotype stain is included as a control. Black bar indicate 2 mm scale



Supplemental Figure 4. *Mof* deletion improves early wound healing. Representative figure showing wound closure in *Lyz2Cre; Mof^{f/f}* and *Mof^{f/f}* control mice on a standard diet. Two wounds were created using 6 mm punch biopsies on the backs of *Lyz2Cre; Mof^{f/f}* or *Mof^{f/f}* mice fed a standard chow diet. Change in wound area was analyzed daily using ImageJ software (n=6 mice/group)



Supplemental Figure 5. *Nos2* expression in DIO wound macrophages is reduced by TNF α inhibition *ex vivo*. Representative figure showing *Nos2* expression in wound macrophages treated with Etanercept *ex vivo*. Wound macrophages (CD11b⁺CD3⁻ CD19⁻Ly6G⁻) were isolated on day 5 post-injury from DIO mice and stimulated *ex vivo* with 250 mg/ml Etanercept or vehicle for 12 hours. *Nos2* expression was measured by qPCR. Data was analyzed using a 1-tailed Student's *t*-test with Welch's correction.



Supplemental Figure 6. Etanercept treatment has no effect on expression of anti-inflammatory genes in DIO wound macrophages. Representative figure showing anti-inflammatory gene expression in wound macrophages treated with Etanercept *ex vivo*. Wound macrophages (CD11b⁺CD3⁻ CD19⁻Ly6G⁻) were isolated on day 5 post-injury from DIO mice and stimulated *ex vivo* with 250 mg/ml Etanercept or vehicle for 12 hours. *Il10*, *Arg1*, and *Ym1* expression was measured by qPCR. Data was analyzed using a 1-tailed Student's *t*-test with Welch's correction.

Patient Characteristic	Non-diabetic	Diabetic
Age	73.3 (10.9)	64.3 (3.2)
Male	100%	50%
BMI	28.3 (1.6)	31.2 (1.8)
Prior Tobacco Use	66%	83%
Diabetes	N/A	100%
Hgb A1c	N/A	8.4 (0.3)
Hypertension	100%	83%
Hyperlipidemia	66%	83%
Coronary Artery Disease	33%	17%
Medications		
Insulin Dependent	N/A	33%
Oral Hyperglycemic	N/A	66%
Immunosuppressants	0%	0%

Supplemental Table 1: Metadata table of patient groups used in this study.

BMI, body mass index; Hgb A1c, hemoglobin A1C; N/A, non-applicable.

Continuous variables expressed as mean (SEM) and categorical variables expressed as percentages.